

**Algae Settlement Inactivates Lanthanum/aluminum Co-modified Attapulgite:  
Implications for Phosphorus Control in Shallow Lakes**

Ming Kong<sup>a,1</sup>, Tianlun Han<sup>a,1</sup>, Hongbin Yin<sup>b</sup>, Xueting Xu<sup>a</sup>, Tao Zhang<sup>a</sup>, Ting Chen<sup>a</sup>, Gang Pan<sup>c</sup>,  
Wenqing Shi<sup>d,\*</sup>, Daming Wei<sup>e,\*</sup>

<sup>a</sup> Nanjing Institute of Environmental Sciences, Ministry of Ecology and Environment, No. 8  
Jiangwangmiao Street, Nanjing 210042, China.

<sup>b</sup> State Key Laboratory of Lake Science and Environment, Nanjing Institute of Geography and  
Limnology, Chinese Academy of Sciences, People's Republic of China.

<sup>c</sup> School of Animal, Rural and Environmental Sciences, Nottingham Trent University,  
Brackenhurst Campus, Southwell NG25 0QF, United Kingdom.

<sup>d</sup> Jiangsu Collaborative Innovation Center of Atmospheric Environment and Equipment  
Technologies, Jiangsu Key Laboratory of Atmospheric Environmental Monitoring & Pollution  
Control, School of Environmental Science & Engineering, Nanjing University of Information  
Science & Technology, Nanjing, 210044, China.

<sup>e</sup> Chinese Academy of Environmental Planning, Ministry of Ecology and Environment, Beijing,  
100012, China.

**\*Corresponding authors:** Wenqing Shi (shiwenqing2005320@126.com) or Daming Wei  
(weidm@caep.org.cn)

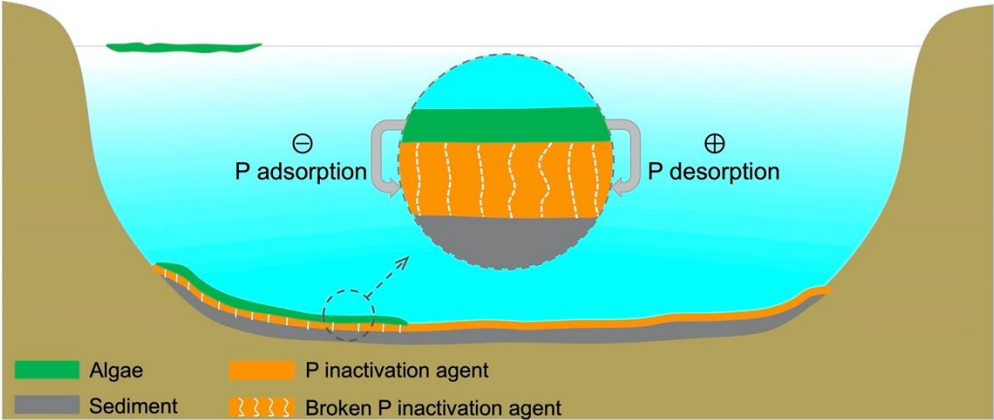
<sup>1</sup> These authors contributed equally to the paper

## **Abstract**

Phosphorus (P) inactivation agents have been widely used to control sediment P release for combating lake eutrophication. The settlement and decomposition of algal biomass from the overlying water can alter the micro-environment of the capping layer and potentially affect the performance of P inactivation agents. In this study, we explored the impacts of algae decomposition on the performance of lanthanum/aluminum co-modified attapulgite (LAA), a commonly used P inactivation agent, and the underlying mechanisms through incubation experiments. The results showed that algae settlement and decomposition could inactivate LAA. After algae settlement, the amount of P locked in the LAA decreased by 11.8% relative to the control. Algae decomposition induced anoxia in the capping layer of LAA, which favored the growth of phosphate solubilizing bacteria, thereby enhancing P release; meanwhile, driven by algae decomposition, more organic matter penetrated the capping layer and competed with P adsorption sites. The increased desorption ability and decreased adsorption ability inhibited the performance of LAA, increasing the P permeability of the capping layer. This study provides beneficial information for future field applications of P inactivation agents for lake restoration.

**Keywords:** phosphorus inactivation agent; algae; organic matter; lake; sediment

**Synopsis:** Algae settlement inactivates sediment phosphorus inactivation agents for combating lake eutrophication.



## Introduction

Lake eutrophication is mainly caused by the over-enrichment of phosphorus (P) in lake water. The main sources of P in lake water are external P inputs and sediment P release (internal P loading). Internal P loadings have been reported to be capable of supporting lake eutrophication for several decades without external P loadings.<sup>1-4</sup> Therefore, the control of internal P loading is a key to combat lake eutrophication. Thus far, several technologies have been developed to reduce internal P loadings.<sup>5-9</sup> With the advantages of easy operation and high efficiency, *in-situ* sediment inactivation is commonly used to control internal P loadings.<sup>10-12</sup> Through sediment inactivation, mobile P can be converted into inert forms, thereby reducing sediment P release.<sup>13-15</sup> For example, more than 25% of mobile P can be transformed into inert P in the top 4 cm of the sediment layer after sediment inactivation.<sup>16</sup> At present, lanthanum and/or aluminum modified clays have been widely used as P-inactivation agents in the field.<sup>17,18</sup> In large lakes, algae may migrate from other zones by winds and settle in the application field of P inactivation agents.<sup>19,20</sup> In Taihu Lake, a Chinese eutrophic lake, dense algal mats are often observed in the downwind northwestern bays following prevailing southeast winds, where many lake geo-engineering measures were conducted to combat algae blooms.<sup>21,22</sup> The decomposition of the settled algal biomass can alter lake micro-environments (pH, ORP, DO, etc.) and consequently change the behavior of P in surface sediments.<sup>23,24</sup> The decomposition of algal biomass has been proven to be capable of transforming sediment organic P (OP) to inorganic P (IP), altering internal P release.<sup>25,26</sup> Moreover, it has been also proven that the decomposition of algal biomass can increase the abundance of P solubilizing bacteria, such as *genus Pseudomonas*, enhancing P release through dissolution.<sup>27</sup> Hence, we hypothesize that,

after the application of P inactivation agents, the decomposition and settling of algal biomass from the overlying water may negatively impact the performance of P inactivation agents, decreasing its ability to control sediment P release.

In this study, we conducted incubation experiments to explore the impacts of algae decomposition on the performance of P inactivation agents. The objectives of this study are to: (i) identify the impacts of algae decomposition on the ability of P inactivation agents to control sediment P release, (ii) explore the underlying mechanisms, and (iii) provide guidance for field applications of P inactivation agents in the future.

## **Material and Methods**

**Preparation of P Inactivation Agents.** In this work, lanthanum/aluminum co-modified attapulgite (LAA), a commonly used P inactivation agent, was studied, which was prepared according to Yin et al. (2020).<sup>9</sup> Clay materials were collected from Xuyi County, Jiangsu Province, China. The prepared LAA was characterized using X-ray fluorescence spectroscopy (XRF-1800, Shimadzu corporation, Japan) and X-ray Diffraction (XRD, Thermo Fisher, USA) (Table S1).

**Incubation Experiments.** Sediment and water samples were collected from Zhushan Bay of Lake Taihu. Located in the Yangtze River Delta, Lake Taihu is the third largest freshwater lake in China with an area of 2,338 m<sup>2</sup> and a mean depth of 1.9 m. In the past decades, large amounts of industrial and domestic wastewater have been discharged into Lake Taihu, causing serious eutrophication and algae blooms. In June 2019, fresh algae slurries, water (20 L), and sediments (20 kg) were collected from Zhushan Bay (31°32'13"N, 120°10'19"E). After being transported to the laboratory, algae slurries were concentrated with a plankton net (250 mesh), and then

freeze-dried; sediment samples were sieved with a 0.2-mm sieve to remove larger stones, organic debris, benthic organisms and garbage, and then fully homogenized before use; water samples were filtered through a filter membrane with a pore size of 0.45  $\mu\text{m}$  to remove impurities and algae.

Incubation experiments were carried out in twenty 5 L-glass beakers. The beakers were divided into four groups ( $n = 5$ ): (i) run with no addition (termed “Control”); (ii) run with only LAA capping (termed, “L-O”); (iii) run with only algae decomposition (termed “A-O”); (iv) run with LAA capping and algae decomposition (termed “L-A”). The beakers were prepared as follows: 400 g of fresh sediments (approximately 5 cm thick) was added to each beaker, and then LAA was added to L-O and L-A treatments. To completely control internal P release and precisely explore the impacts of algae decomposition, a higher dosage of LAA was added relative to the theoretical minimum dosage, which was calculated according to Yin et al. (2020).<sup>9</sup> In the A-O and L-A treatments, 2 g of freeze-dried algae was added. Finally, 1000 mL water was carefully poured into the beaker along the tube wall by siphoning. When algal accumulation occurs, light hardly reaches bed sediments under dense algal canopies,<sup>28</sup> these sediment cores were therefore incubated in the dark in an incubator under constant temperature (25°C). On days 0, 7, 15, 22, and 30, dissolved oxygen (DO), ORP, and pH in the overlying water were determined using a multi-sensor probe (YSI 6600, Yellow Springs Instruments, USA). On days 15 and 30, overlying water (50 mL) was collected for excitation emission matrix fluorescence analysis; surface sediments (100 g) and LAA in the capping layer (10 g) were collected for the analyses of P fractions and microbes.

**Organic Matter Characterization.** Organic matter in the overlying water was characterized

by fluorescence excitation-emission matrix (EEM) spectroscopy (Hitachi High Technologies, Tokyo, Japan). The EEM spectra were collected with scanning emission (Em) spectra from 250 to 550 nm at 5 nm increments by varying the excitation (Ex) wavelength from 250 to 450 nm at 5 nm increments. The soluble organic matters at the specific fluorescence peak were identified according to Baghoth et al. (2008) and Derrien et al. (2017).<sup>29,30</sup>

**Sediment Microbial Analysis.** The surface sediment (0–1 cm) and LAA in the capping layer were stored at -80°C prior to high-throughput sequencing analysis. DNA extraction was conducted using a FastDNA Power-Max Soil DNA Isolation Kit (MP Biomedical, USA) according to the manufacturer's instructions. The detection and analysis of DNA information was conducted by Covaris M220. Beta diversity differences between samples were calculated using Mothur software.<sup>31</sup>

**Sediment P Fraction Analysis.** Sediment IP fractions were analyzed using the continuous extraction method.<sup>32</sup> The sequential extraction was as follows: 1 mol/L NH<sub>4</sub>Cl solution at pH = 7, 0.11 mol/L Na<sub>2</sub>S<sub>2</sub>O<sub>4</sub>/0.11 mol/L NaHCO<sub>3</sub> solution, 0.1 mol/L NaOH solution, 0.5 mol/L HCl solution, and finally 1 mol/L NaOH at 358K, the measured P fraction of which was referred to as labile-P, BD-P, NaOH-rP and NaOH-nrP, HCl-P and Residual-P, respectively. The sum of labile-P, BD-P and NaOH-nrP is mobile-P. Sediment OP fractions were analyzed using the modified method.<sup>33</sup> The labile organic P (LOP) was extracted with 0.5 M NaHCO<sub>3</sub> at pH = 8.5. The moderately labile organic P (MLOP) was extracted with 1 mol/L HCl, and then treated with 0.5 mol/L NaOH. The NaOH extract was acidified to pH = 0.2 using HCl. Humic-Po and Fulvic-Po were separated into supernatant and precipitate, respectively. The non-labile organic P (NOP) was obtained by ashing the solid residue from NaOH extraction at 550°C for 1 h and

subsequently dissolving it in 1 mol/L H<sub>2</sub>SO<sub>4</sub>.

Prior to <sup>31</sup>P NMR analysis (Bruker AV500, Bruker Co., Switzerland), samples were prepared as follows: 2 g sediment was extracted with a solution of 0.05 mol/L EDTA in 0.25 mol/L NaOH at 1:8 (m:v) ratio for 16 h at 20°C. An aliquot of extract was taken for TP and IP analysis, while the remaining solution was freeze-dried until the volume reached 10% of the initial, and then stored at -20°C before <sup>31</sup>P NMR analysis.<sup>34,35</sup> Before recording the NMR spectra, the precipitate was freshly separated from solution using a centrifuge (10,000 rpm for 10 min). An aliquot of D<sub>2</sub>O was added into the solution for signal lock. The standard cavity 5 mm BBO probe was used. The <sup>31</sup>P spectrum was recorded using the following program: resonance 242.739 MHz, pulse time 5.9 s, cycle delay 3 s, and taking 20,000 scans at 20°C. All <sup>31</sup>P chemical shifts refer to 85% H<sub>3</sub>PO<sub>4</sub>, and MestReNova software was used for signal processing.

**Statistical Analysis.** Statistically significant differences between treatments were tested using one-way analysis of variance (ANOVA) with post-hoc multiple comparisons. For normality, the Kolmogorov-Smirnov and variance homogeneity tests were conducted prior to analysis of variance. Logarithmic transformation was also conducted and the transformed data were examined to ensure satisfaction of ANOVA assumptions. The level of statistical significance was set at  $p < 0.05$ . All these statistical calculations were performed using SPSS 22.0 (SPSS Inc., North Chicago, IL, USA).

## Results

**Water DO and ORP.** In the control, DO in the overlying water remained at  $3.70 \pm 0.11$  mg/L throughout the experiment. The LAA in the L-O treatment significantly increased DO ( $p < 0.05$ ), whereas algae decomposition in the A-O treatment consumed oxygen and significantly



decreased DO ( $p < 0.05$ ), which reached below 2 mg/L after 15 days (Figure 1a). During the entire experiment, the ORP of the overlying water decreased in the control. The LAA capping significantly increased ORP ( $p < 0.05$ ), but algae decomposition weakened the effect; in contrast, with only algae decomposition, ORP declined dramatically. At the end of the experiment, the ORP of the overlying water decreased from  $126.33 \pm 2.67$  to  $83.67 \pm 3.24$ ,  $118.30 \pm 3.57$ ,  $47.97 \pm 1.89$ , and  $102.70 \pm 1.88$  mV in the control, L-O, A-O, and L-A treatments, respectively (Figure 1b).

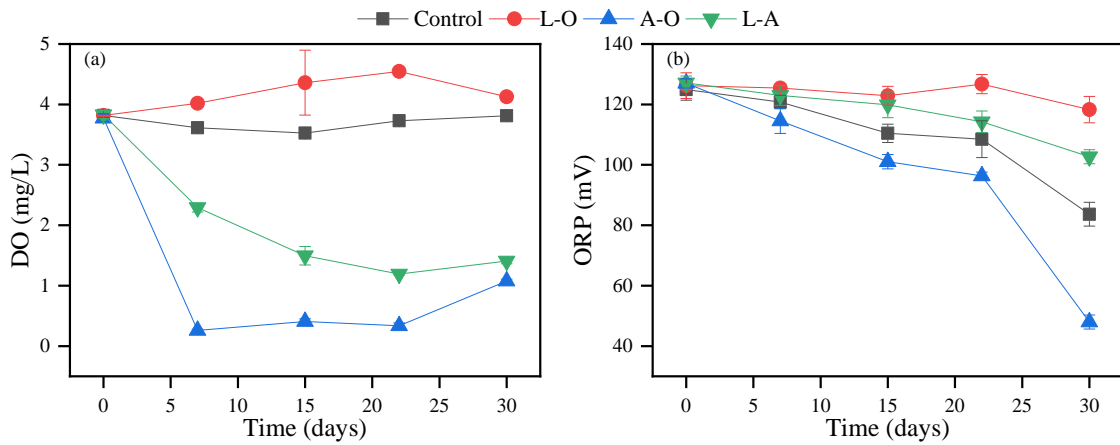


**Figure 1.** Changes of DO and ORP in the overlying water throughout incubation experiments.

(a) DO; (b) ORP. Error bars indicate standard deviations.

**Water Fluorescence EEM Spectra.** According to parallel factor (PARAFAC) analysis, four main peaks were identified in the overlying water (Figure 2a-d). Component 1 (Ex/Em: 250-295/400) and Component 3 (Ex/Em: 275-360/445) correspond to microbial humic-like substances and terrestrial humic-like substances, respectively. Component 2 (Ex/Em: 275/320) and Component 4 (Ex/Em: 255/350) correspond to typical protein-like substances. The fluorescence intensity of each component is shown in Figure 3. Compared with the control (1.24 R.U.), the average fluorescence intensity of Component 1 increased to 2.28 R.U. in the A-O treatment, and decreased to 0.17 R.U. in the L-O treatment, but showed no significant

differences between the L-O and L-A treatments ( $p > 0.05$ ) (Figure 3a). Compared with the control (1.62 R.U.), the average fluorescence intensities of Components 2 and 3 increased to 3.83 and 2.54 R.U. in the A-O treatment and further increased to 4.88 and 8.21 R.U. in the L-A treatment, respectively (Figure 3b, c). In contrast, Component 4 was not detected in the control and A-O treatment, but showed high levels in treatments with LAA capping. On day 30, the fluorescence intensity of Component 4 was 0.01, 2.00, 0, and 1.70 R.U. in the control, L-O, A-O, and L-A treatments, respectively (Figure 3d).

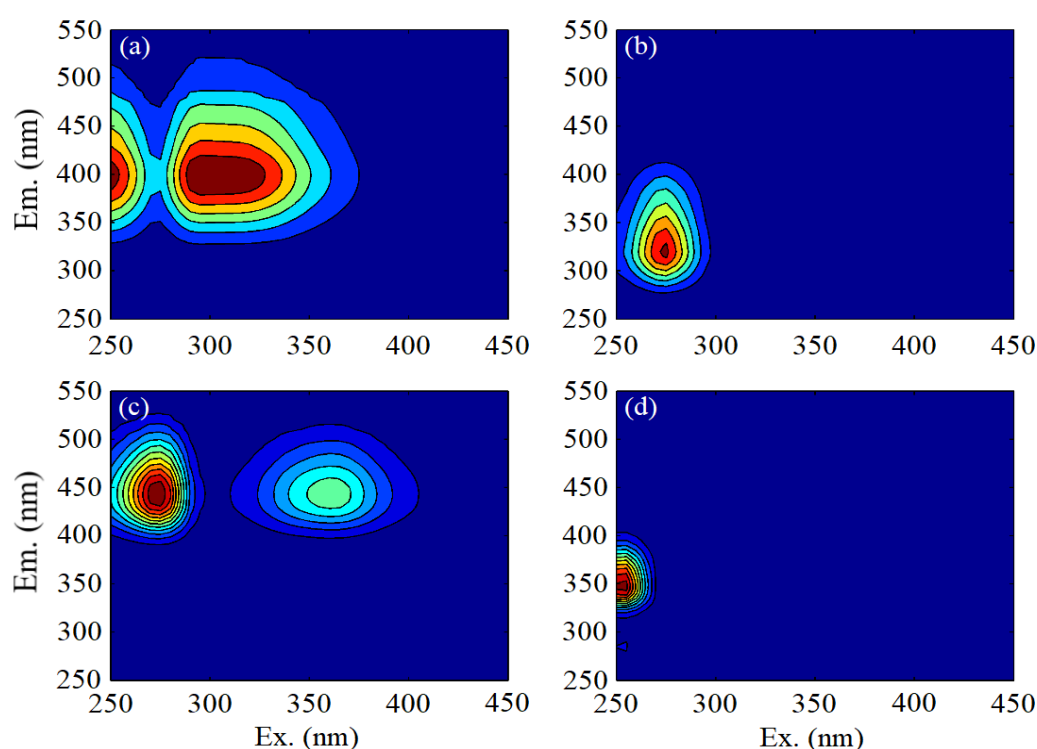


**Figure 2.** Water excitation-emission matrix fluorescence spectra. (a) Component 1; (b) Component 2; (c) Component 3; (d) Component 4.

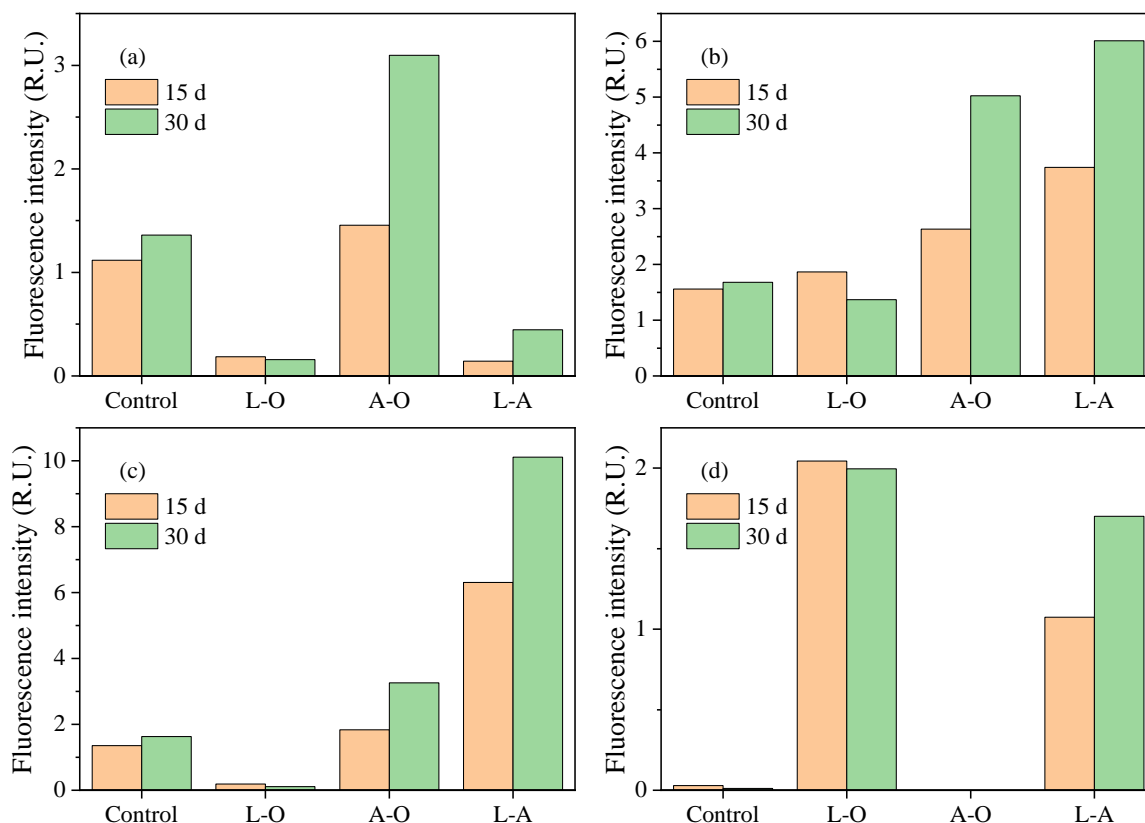


**Figure 3.** Fluorescence intensity of different organic matters in the overlying water. (a) Component 1; (b) Component 2; (c) Component 3; (d) Component 4.

**Microbial Community Structure.** Heatmap of Bray Curtis, Weighted Unifrac, and Unweighted Unifrac distances of microbes are presented in Figure S1. Sediments in the A-O treatment and LAA in the L-O treatment exhibited the largest distance values (0.919, 0.693, 0.530). In the L-O and L-A treatments, although sediments exhibited small distance values (0.431, 0.228, 0.244), the LAA exhibited larger distance values (0.884, 0.560, 0.485). As shown in Figure 4, *Bacteroidetes*, *Firmicutes*, and *Proteobacteria* were the dominant species with relative abundances of 19.59–43.56%, 16.77–39.20%, and 9.67–30.98%, respectively. With reference to the control (24.11%), the relative abundance of *Bacteroidetes* in surface sediments decreased to 19.37% in L-O and increased to 34.94% in A-O. Within the capping layer, algae decomposition increased the relative abundance of *Bacteroidetes* by approximately 3.3%, but

it increased the abundance of phosphate solubilizing bacteria (*Firmicutes*, *Proteobacteria*, and *Bacteroidetes*). Compared with the control, the LAA capping decreased the relative abundance of phosphate solubilizing bacteria, but algae decomposition increased their abundance by approximately 19%. In addition, the relative abundance of phosphate solubilizing bacteria in both surface sediments and the capping layer in the L-A treatment was higher than that in the L-O treatment.

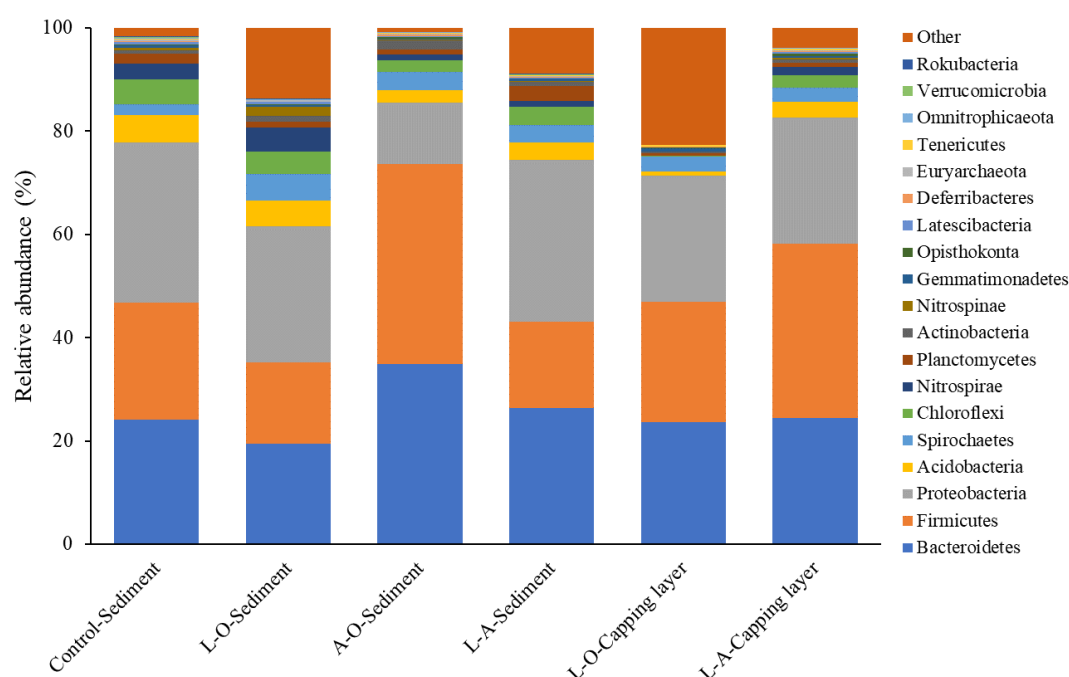


**Figure 4.** The relative abundance of microbial phylum in samples.

**LAA in the Capping Layer.** In the XRD spectra (Figure 5a), the peaks at  $2\theta = 25.52^\circ$  and  $2\theta = 27.46^\circ$  were absent in the L-A treatment. These two peaks were identified as  $\text{KAlSi}_3\text{O}_8$ , which is responsible for P adsorption. We found that TP in the capping layer increased to  $210.9 \pm 10.5$  mg/kg on day 15 and to  $220.8 \pm 13.7$  mg/kg on day 30 in the L-O treatment. In contrast, TP in the capping layer decreased to  $194.32 \pm 10.41$  mg/kg (11.8% decrease) in the L-A treatment (Figure 5b).

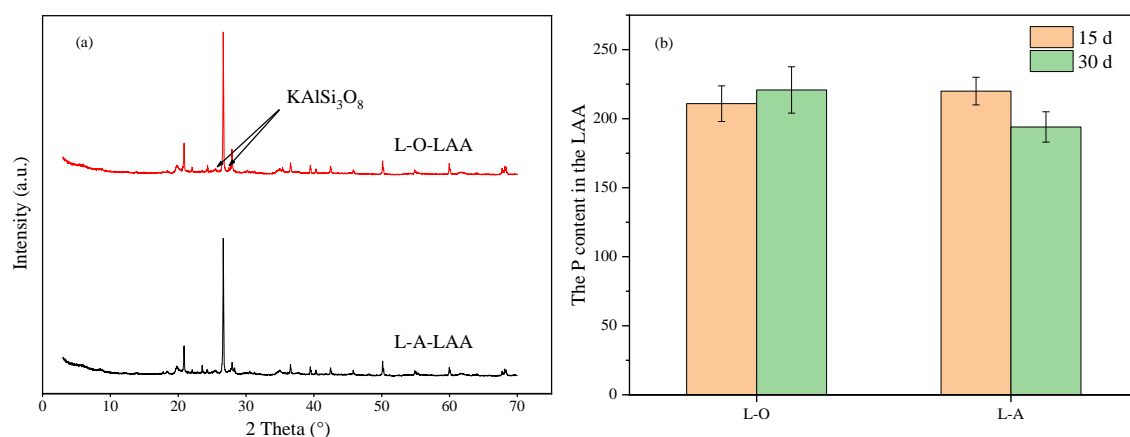
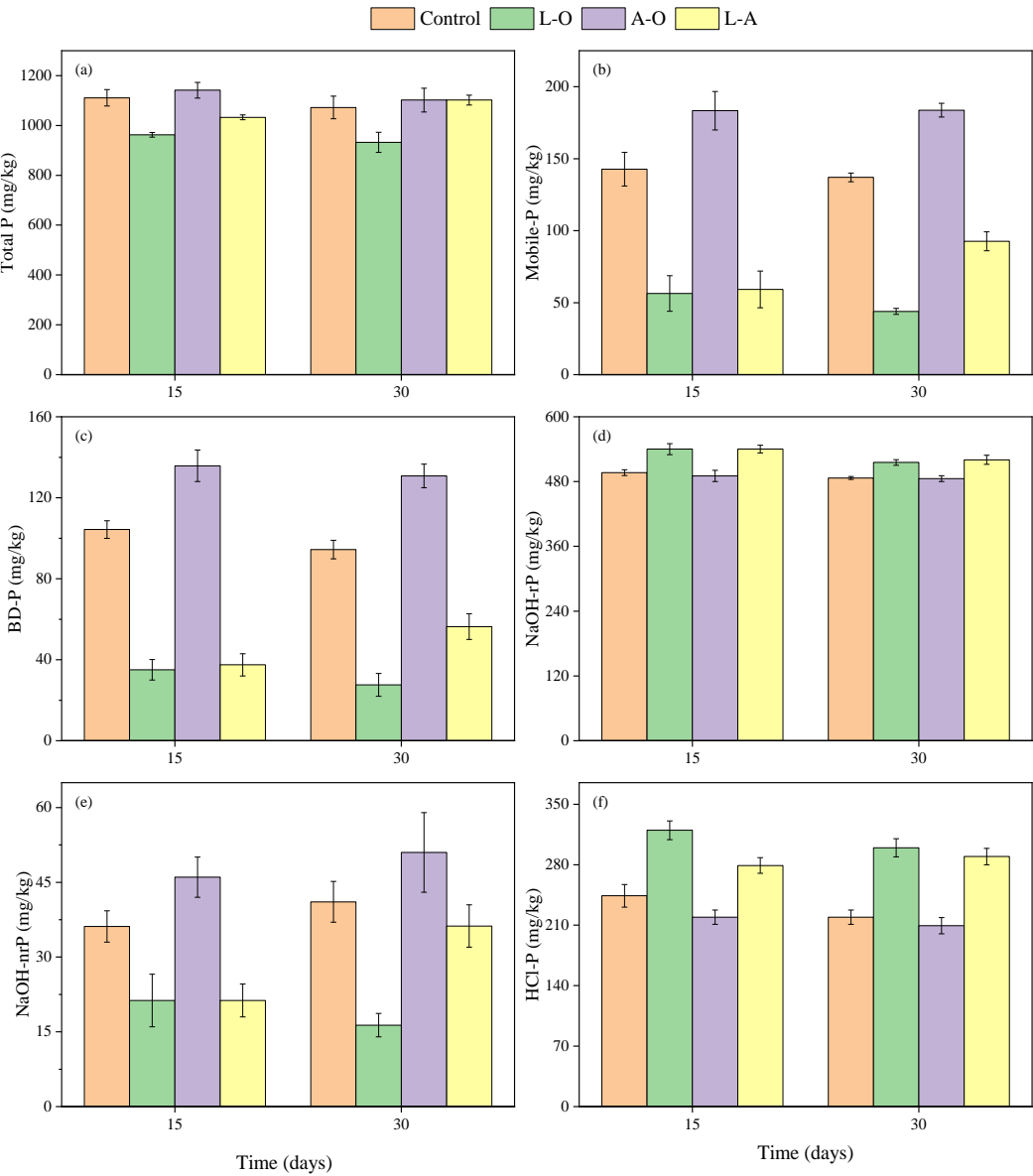


**Figure 5.** Changes of LAA in the capping layer throughout the incubation experiment. (a) XRD analysis; (b) TP. Error bars indicate standard deviations.

**Sediment IP Fractions.** With reference to the control ( $1072.3 \pm 37.0$  mg/kg on day 30), the LAA capping in the L-O treatment decreased sediment TP to  $932.7 \pm 32.9$  mg/kg. In contrast, algae settlement and decomposition in the L-A treatment slightly increased sediment TP to  $1101.9 \pm 39.1$  mg/kg (Figure 6a). IP fraction analysis indicated that LAA capping significantly decreased Mobile-P ( $p < 0.01$ ). On day 30, sediment Mobile-P in the L-O treatment was 67.9% less than that in the control, of which BD-P content dropped by approximately 66%. Algae settlement and decomposition dramatically increased sediment Mobile-P (Figure 6b); in the A-O treatment, BD-P and NaOH-nrP increased by approximately 34% and 25%, respectively. Moreover, algae settlement and decomposition after the application of LAA capping could also increase Mobile-P in sediments below the capping layer. On day 30, sediment Mobile-P in the L-A treatment increased to almost twice that in the L-O treatment, with BD-P and NaOH-nrP increasing by 50% and 70%, respectively (Figure 6c-e). Sediment HCl-P increased and decreased with the LAA capping and algae settlement and decomposition, respectively. In the control and the L-O, A-O, and L-A treatments, sediment HCl-P was  $244.1 \pm 10.7$ ,  $319.9 \pm 8.9$ ,  $219.3 \pm 6.8$ , and  $279.1 \pm 7.4$  mg/kg on day 15, and  $219.3 \pm 6.8$ ,  $299.5 \pm 8.6$ ,  $209.4 \pm 7.7$ , and

224     289.5 ± 7.8 mg/kg on day 30, respectively (Figure 6f).



225  
226     **Figure 6.** Changes of IP fractions in the sediment throughout the experiment. (a) TP; (b)  
227     Mobile-P; (c) BD-P; (d) NaOH-rP; (e) NaOH-nrP; (f) HCl-P. Error bars indicate standard  
228     deviations.

229     **Sediment OP Fractions.** With reference to the control, the LAA capping in the L-O treatment  
230     decreased sediment LOP and MLOP by approximately 64% and 32%, respectively (Figure 7a  
231     and b), whereas algae settlement and decomposition in the A-O treatment increased sediment

LOP and MLOP by approximately 11% and 20%, respectively. Algae settlement after the LAA capping in the L-A treatment could also increase sediment LOP and MLOP by approximately 21% and 27%, respectively. Compared with the L-O treatment, NOP content in the L-A treatment increased by approximately 4% (Figure c). Although MLOP content was far lower than NOP content in the L-O and L-A treatments, MLOP content was higher than NOP content in the L-A treatment because of algae decomposition, which suggests that algae decomposition mainly weakened the inactivation effect of LAA on MLOP.

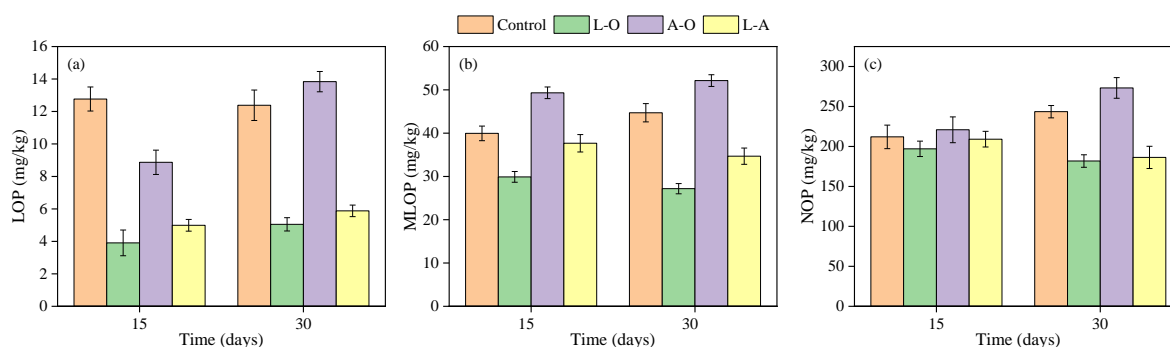


**Figure 7.** Changes of OP fractions in the sediment throughout the experiment. (a) LOP; (b) MLOP; (c) NOP. Error bars indicate standard deviations.

**Sediment Molecular P.** According to  $^{31}\text{P}$ -NMR spectra analysis (Figure S2, Table 1), TP in the NaOH-EDTA extracts was 389.36–638.80 mg/kg, and Ortho-P was the dominant species, which was maintained at 280.64–437.92 mg/kg and accounted for 67.2–72.1%. Pyro-P was only detected in the control and A-O treatment, with contents of 22.96 and 8.40 mg/kg accounting for 3.9% and 1.3%, respectively. Mono-P was the most important OP in NaOH-EDTA extracts, with concentrations of 98.40–155.52 mg/kg accounting for 23.9–25.3% in  $\text{TP}_{\text{NaOH-EDTA}}$ . Compared with the L-O treatment, the concentration of Mono-P in  $\text{TP}_{\text{NaOH-EDTA}}$  was lower in the L-A treatment. The concentrations of DNA-P were 10.32–36.96 mg/kg, accounting for 2.7–5.8% of  $\text{TP}_{\text{NaOH-EDTA}}$ . Phosphonates were detected only in the control with

an extremely low concentration of 1.68 mg/kg, accounting for 0.3% of TP<sub>NaOH-EDTA</sub>. Compared with the control, higher concentrations of DNA-P and Mono-P were detected in the A-O treatment, indicating larger production of OP due to algae decomposition. The concentrations of DNA-P and Mono-P were 27.84 mg/kg and 140.80 mg/kg in the control, and 36.96 mg/kg and 155.52 mg/kg in the A-O treatment.

**Table 1** P fractions in the NaOH-EDTA extracts from surface sediments

Treatment	TP <sub>NaOH-EDTA</sub> mg/kg	Pi		Po		
		Ortho-P	Pyro-P	mono-P	DNA-P	Phon-P
Control	589.36 (55.0%) <sup>b</sup>	396.08 (67.2%) <sup>c</sup>	22.96 (3.9%)	140.80 (23.9%)	27.84 (4.7%)	1.68 (0.3%)
L-O	389.36 (41.7%)	280.64 (72.1%)	n.d.	98.40 (25.3%)	10.32 (2.7%)	n.d.
A-O	638.80 (58.0%)	437.92 (68.6%)	8.40 (1.3%)	155.52 (24.3%)	36.96 (5.8%)	n.d.
L-A	459.20 (41.7%)	326.24 (71.0%)	n.d.	111.20 (24.2%)	21.76 (4.7%)	n.d.

n.d. not detected.

<sup>a</sup> The value was calculated from the concentration in the NaOH-EDTA extract and dry weight.

<sup>b</sup> The proportion of TP in NaOH-EDTA extracts to TP in sediments (%).

<sup>c</sup> The proportion of each P fraction to TP in NaOH-EDTA extract.

## Discussion

After settlement, algae die and decompose, consuming oxygen at the sediment surface and physically preventing oxygen diffusion into the sublayer.<sup>36-38</sup> Thus, in the A-O and L-A treatments, the DO in the overlying water exhibited a sharp decline, which induced an anaerobic environment in the capping layer (Figure 1a and b). The anoxia reshaped microbial



communities and favored the growth of phosphate solubilizing bacteria (Figure 4) and P mineralization bacteria.<sup>27,39</sup> Phosphate solubilizing bacteria can transform insoluble P into soluble P for biological absorption and utilization through their own metabolisms or synergistic effects with other organisms.<sup>40</sup> Therefore, the increased abundance of phosphate solubilizing bacteria could promote the transformation of insoluble inert-P to mobile-P (Figure 6b). Organic P mineralization bacteria could transform HCl-P and promote the formation of BD-P and NaOH-nrP under anaerobic conditions, which could increase the content of mobile-P in sediments.<sup>27,41</sup> Further correlation analysis indicated a negative correlation between BD-P and HCl-P ( $p < 0.01$ ). In fields, water column is difficult to be anoxia due to frequent disturbances induced by winds,<sup>42</sup> but we argue algae settlement may remarkably affect oxygen penetrated into sediments and control P biogeochemical cycles, which need further studies using the oxygen microelectrode system.

Algae decomposition involves the release of large amounts of organic matter,<sup>43,44</sup> which penetrate the P inactivation agent capping layer.<sup>17</sup> Moreover, algae-induced anoxia could also enhance organic matter release from sediments. The PARAFAC analysis revealed a significant increase in terrestrial humic-like substances in the L-A treatment, which indicates that algae settlement and decomposition not only released organic matter (Figure 3c), but also promoted organic matter release from sediments. The different fluorescence intensities between the L-A and L-O treatments indicate that P inactivation agents adsorbed a large amount of organic matter. This may have negative impacts on the P absorption ability of P inactivation agents because organic matter could compete with P absorption sites.<sup>45</sup> The weakened adsorption ability is firmly supported by the disappearance of P adsorption sites in P inactivation agents

after algae settlement (Figure 5a).

The enhanced P desorption and weakened P absorption decreased the ability of P inactivation agents to lock P. We detected a decrease in the P content of P inactivation agents after algae settlement, and P could easily pass through the capping layer. Therefore, sediments below the capping layer showed high P content in the L-A treatment (Figure 6a). This also agrees with the fluorescence intensity analysis (Figure 3b and c). The algae decomposition produced OP (such as mono-P and DNA-P),<sup>40</sup> which passed through the capping layer and increased the OP content in sediments (Figure 6d). The ratio of Mono-P in sediments was lower in the A-O and L-A treatments than in the L-O treatment (Table 1). This is attributable to the enhanced mineralization of OP in sediments due to algae decomposition and the transformation of OP to Ortho-P<sup>46</sup>. The anaerobic environment and algae decomposition increased the content of mobile-P in sediments (Figure 6b), weakening the ability of P inactivation agents to deactivate the increased mobile-P, which in turn weakened the inactivation effect of P inactivation agents. Hence, after the application of P inactivation agents, algae settlement and decomposition changed the properties of P inactivation agents and manipulated microbial communities in the capping layer, weakening the P inactivation effect.

In this study, we found that the decomposition of algal biomass from the overlying water can negatively affect P inactivation agents. As P inactivation agents cannot directly control algae blooms, algae settlement often frequently occurs after sediment capping. Thus, if possible, P inactivation agents should not be applied during algae bloom seasons. Moreover, the dose of P inactivation agents in actual applications should be higher than the theoretical minimum dosage to counteract the potential negative impacts of algae settlement.

## Conclusions

In fields, P inactivation agents has been widely applied to lock P and control sediment P release. After sediment capping, the decomposition of algae biomass from the overlying water can change the micro-environment of the capping layer, potentially affecting the performance of P inactivation agents. In this study, we investigated the impacts of algae decomposition on the performance of P inactivation agents and the underlying mechanisms through incubation experiments. The decomposition of algae biomass depleted oxygen and induced anoxia in the P inactivation agents capping layer, creating favorable conditions for phosphate solubilizing bacteria and enhancing P desorption. Organic matter derived from algae biomass penetrated the capping layer and competed with P absorption sites. The increased P desorption and decreased P absorption inhibit the ability of P inactivation agents to control sediment P release, and P can easily pass through the capping layer. As P inactivation agents cannot directly control algae blooms, algae settlement often frequently occurs after sediment capping. Thus, if possible, P inactivation agents should not be applied during algae bloom seasons. Moreover, the dose of P inactivation agents in field applications should be higher than the theoretical minimum dosage to counteract the potential negative impacts of algae settlement.

## Supporting Information

This material is available free of charge via the internet at <http://pubs.acs.org>.

Physico-chemical properties of lanthanum/aluminum co-modified attapulgite,  $^{31}\text{P}$  NMR spectra of NaOH-EDTA extracts of sediments, Heatmap of sediments and lanthanum/aluminum co-modified attapulgite.

## Acknowledgments

332 This work was financially supported by the Special Fund of Chinese Central Government for  
333 Basic Scientific Research Operations in commonweal Research Institute (GYZX220102),  
334 National Natural Science Foundation of China (41701568 and 51979171), Natural Science  
335 Foundation of Jiangsu Province (BK20171518), State Key Laboratory of Hydrology-Water  
336 Resources and Hydraulic Engineering (2018nkms01), CAS Interdisciplinary Innovation Team  
337 (JCTD-2018-16), and Key Research Program of Frontier Sciences, CAS (ZDBS-LY-DQC018).

## References

1. Smith, V. H.; Schindler, D. W., Eutrophication science: where do we go from here? *Trends Ecol. Evol.* **2009**, *24*, (4), 201-207.
2. Roy, E. D.; Nguyen, N. T.; Bargu, S.; White, J. R., Internal loading of phosphorus from sediments of Lake Pontchartrain (Louisiana, USA) with implications for eutrophication. *Hydrobiologia* **2012**, *684*, (1), 69-82.
3. Paytan, A.; Roberts, K.; Watson, S.; Peek, S.; Chuang, P. C.; Defforey, D.; Kendall, C., Internal loading of phosphate in Lake Erie Central Basin. *Sci. Total Environ.* **2017**, *579*, 1356-1365.
4. Anderson, H. S.; Johengen, T. H.; Godwin, C. M.; Purcell, H.; Alsip, P. J.; Ruberg, S. A.; Mason, L. A., Continuous In Situ Nutrient Analyzers Pinpoint the Onset and Rate of Internal P Loading under Anoxia in Lake Erie's Central Basin. *ACS ES&T Water* **2021**, *1*, (4), 774-781.
5. Luerling, M.; Faassen, E. J., Controlling toxic cyanobacteria: Effects of dredging and phosphorus-binding clay on cyanobacteria and microcystins. *Water Research* **2012**, *46*, (5), 1447-1459.
6. Spear, B. M.; C., M. S.; G., P.; Mackay, E.; Bruere, A.; Corker, N.; Douglas, G.; Egemose, S.; Hamilton, D.; Hatton-Ellis, T.; Huser, B.; Li, W.; Meis, S.; Moss, B.; Lürling, M.; Phillips, G.; Yasseri, S.; Reitzel, K., Geo-Engineering in Lakes: A Crisis of Confidence? . *Environ. Sci. Technol.* **2014**, *48*, (17), 9977-9979.
7. Mucci, M.; Maliaka, V.; Noyma, N. P.; Marinho, M. M.; Lürling, M., Assessment of possible solid-phase phosphate sorbents to mitigate eutrophication: Influence of pH and anoxia. *Sci. Total Environ.* **2018**, *619*, 1431-1440.

8. Lin, J. W.; He, S. Q.; Zhang, H. H.; Zhan, Y. H.; Zhang, Z. B., Effect of zirconium-modified zeolite addition on phosphorus mobilization in sediments. *Sci. Total Environ.* **2019**, *646*, 144-157.
9. Yin, H.; Yang, P.; Kong, M.; Li, W., Use of lanthanum/aluminum co-modified granulated attapulgite clay as a novel phosphorus (P) sorbent to immobilize P and stabilize surface sediment in shallow eutrophic lakes *Chem. Eng. J.* **2020**, 385.
10. Lin, J.; Zhan, Y.; Zhu, Z., Evaluation of sediment capping with active barrier systems (ABS) using calcite/zeolite mixtures to simultaneously manage phosphorus and ammonium release. *Sci. Total Environ.* **2011**, *409*, (3), 638-646.
11. Yin, H.; Kong, M., Reduction of sediment internal P-loading from eutrophic lakes using thermally modified calcium-rich attapulgite-based thin-layer cap. *J. Environ. Manage.* **2015**, *151*, 178-185.
12. Zhou, J.; Li, D.; Chen, S.; Xu, Y.; Geng, X.; Guo, C.; Huang, Y., Sedimentary phosphorus immobilization with the addition of amended calcium peroxide material. *Chem. Eng. J.* **2019**, *357*, 288-297.
13. Fan, Y.; Li, Y.; Wu, D.; Li, C.; Kong, H., Application of zeolite/hydrous zirconia composite as a novel sediment capping material to immobilize phosphorus. *Water Res.* **2017**, *123*, 1-11.
14. Xu, R.; Zhang, M. Y.; Mortimer, R.; Pan, G., Enhanced Phosphorus Locking by Novel Lanthanum/Aluminum-Hydroxide Composite: Implications for Eutrophication Control *Environ. Sci. Technol.* **2017**, *51*, (6), 3418-3425.
15. Kuster, A. C.; Kuster, A. T.; Huser, B. J., A comparison of aluminum dosing methods for reducing sediment phosphorus release in lakes. *J. Environ. Manage.* **2020**, *261*, 110195.

16. Meis, S.; Spears, B. M.; Maberly, S. C.; Perkins, R. G., Assessing the mode of action of Phoslock in the control of phosphorus release from the bed sediments in a shallow lake (Loch Flemington, UK). *Water Res.* **2013**, *47*, (13), 4460-4473.
17. Yin, H.; Du, Y.; Kong, M.; Liu, C., Interactions of riverine suspended particulate matter with phosphorus inactivation agents across sediment-water interface and the implications for eutrophic lake restoration. *Chem. Eng. J.* **2017**, *327*, 150-161.
18. Li, X. D.; Xie, Q.; Chen, S. H.; Xing, M. C.; Guan, T.; Wu, D. Y., Inactivation of phosphorus in the sediment of the Lake Taihu by lanthanum modified zeolite using laboratory studies. *Environ. Pollut.* **2019**, *247*, 9-17.
19. Chen, M.; Ding, S.; Chen, X.; Sun, Q.; Fan, X. F.; Lin, J.; Ren, M. Y.; Yang, L. Y.; Zhang, C. S., Mechanisms driving phosphorus release during algal blooms based on hourly changes in iron and phosphorus concentrations in sediments. *Water Res.* **2018**, *133*, 153-164.
20. Zhu, L.; Shi, W. Q.; Dam, B. V.; Kong, L. W.; H., Y. J.; Qin, B. Q., Algal Accumulation Decreases Sediment Nitrogen Removal by Uncoupling Nitrification-Denitrification in Shallow Eutrophic Lakes. *Environ. Sci. Technol.* **2020**, *54*, (10), 6194-6201.
21. Deng, J.; Chen, F.; Liu, X.; Peng, J.; Hu, W., Horizontal migration of algal patches associated with cyanobacterial blooms in an eutrophic shallow lake. *Ecol. Eng.* **2016**, *87*, 185-193.
22. Pan, G.; Yang, B.; Wang, D.; Chen, H.; Tian, B. H.; Zhang, M. L.; Yuan, Z. X.; Chen, J., In-lake algal bloom removal and submerged vegetation restoration using modified local soils. *Ecol. Eng.* **2011**, *37*, (2), 302-308.
23. Han, C.; Ding, S. M.; Yao, L.; Shen, Q. S.; Zhu, C. G.; Wang, Y.; Xu, D., Dynamics of

phosphorus–iron–sulfur at the sediment–water interface influenced by algae blooms decomposition %J Journal of Hazardous Materials. *Hazard. Mater.* **2015**, *300*, 329-337.

24. Zhang, W.; Gu, P.; Zhu, W.; Jing, C.; He, J.; Yang, X.; Zhou, L.; Zheng, Z., Effects of cyanobacterial accumulation and decomposition on the microenvironment in water and sediment *J. Soil. Sediment.* **2020**, *20*, (5), 2510-2525.

25. Chen, M.; Ye, T. R.; Krumholz, L. R.; Jiang, H. L., Temperature and Cyanobacterial Bloom Biomass Influence Phosphorous Cycling in Eutrophic Lake Sediments. *PLOS ONE* **2014**, *9*, (3), e93130.

26. Hu, M. J.; Peñuelas, J.; Sardans, J.; Tong, C.; Chang, C. T.; Cao, W. Z., Dynamics of phosphorus speciation and the phoD phosphatase gene community in the rhizosphere and bulk soil along an estuarine freshwater-oligohaline gradient. *Water Res.* **2020**, *365*, 114236.

27. Wang, Z. C.; Huang, S.; Li, D. H., Decomposition of cyanobacterial bloom contributes to the formation and distribution of iron-bound phosphorus (Fe-P): Insight for cycling mechanism of internal phosphorus loading. *Sci. Total Environ.* **2019**, *652*, 696-708.

28. Thomsen, M. S., De Bettignies, T., Wernberg, T., Holmer, M., Debeuf, B., Harmful algae are not harmful to everyone. *Harmful Algae* **2012**, *16*, 74-80.

29. Baghoth, S.; Maeng, S.; Rodriguez, S. S.; Ronteltap, M.; Sharma, S.; Kennedy, M.; Amy, G., An urban water cycle perspective of natural organic matter (NOM): NOM in drinking water, wastewater effluent, storm water, and seawater. *Water Science and Technology: Water Supply* **2008**, *8*, (6), 701-707.

30. Derrien, M.; Lee, Y. K.; Park, J.-E.; Li, P.; Chen, M.; Lee, S. H.; Lee, S. H.; Lee, J.-B.; Hur, J., Spectroscopic and molecular characterization of humic substances (HS) from soils and



426 sediments in a watershed: comparative study of HS chemical fractions and the origins.  
 427 *Environmental Science and Pollution Research* **2017**, *24*, (20), 16933-16945.

428 31. Hamady, M.; Lozupone, C.; Knight, R., Fast UniFrac: facilitating high-throughput  
 429 phylogenetic analyses of microbial communities including analysis of pyrosequencing and  
 430 PhyloChip data. *ISME J.* **2010**, *4*, (1), 17-27.

431 32. Wang, C.; He, R.; Wu, Y.; Lüring, M.; Cai, H.; Jiang, H.; Liu, X., Bioavailable phosphorus  
 432 (P) reduction is less than mobile P immobilization in lake sediment for eutrophication control  
 433 by inactivating agents. *Water Res.* **2017**, *109*, 196-206.

434 33. Ivanoff, D. B.; Reddy, K. R.; Robinson, S., Chemical fractionation of organic phosphorus  
 435 in selected histosols. *Soil Sci.* **1998**, *163*, 36-45.

436 34. Hupfer, M.; Rube, B.; Schmieder, P., Origin and diagenesis of polyphosphate in lake  
 437 sediments: A <sup>31</sup>P-NMR study. *Limnol. Oceanogr.* **2004**, *49*, (1), 1-10.

438 35. Turner, B. L., Optimizing Phosphorus Characterization in Animal Manures by Solution  
 439 Phosphorus-31 Nuclear Magnetic Resonance Spectroscopy. *J. Environ. Qual.* **2004**, *33*, (2),  
 440 757-766.

441 36. Trimmer, M.; Nicholls, J. C.; Deflandre, B., Anaerobic Ammonium Oxidation Measured  
 442 in Sediments along the Thames Estuary, United Kingdom. *Appl. Environ. Microbiol.* **2003**, *69*,  
 443 (11), 6447-6454.

444 37. Vopel, K.; Gibbs, M.; Hickey, C. W.; Quinn, J., Modification of sediment–water solute  
 445 exchange by sediment-capping materials: effects on O<sub>2</sub> and pH. *Ma. Freshwater Res.* **2008**, *59*,  
 446 (12), 1101-1110.

447 38. Smolders, E.; Baetens, E.; Verbeeck, M.; Nawara, S.; Diels, J.; Verdievel, M.; Peeters, B.;

448 Cooman, W. D.; Baken, S., Internal Loading and Redox Cycling of Sediment Iron Explain  
 449 Reactive Phosphorus Concentrations in Lowland Rivers. *Environ. Sci. Technol.* **2017**, *51*, (5),  
 450 2584-2592.

451 39. Maitra, N., Manna, S. K., Samanta, S., Sarkar, K., Debnath, D., Bandopadhyay, C., Sahu,  
 452 S. K., Sharma, A. P., Ecological significance and phosphorus release potential of phosphate  
 453 solubilizing bacteria in freshwater ecosystems. *Hydrobiologia* **2014**, *745*, 69-83.40.

454 40. Zhang, W.; Zhu, X.; Jin, X.; Meng, X.; Tang, W.; Shan, B., Evidence for organic phosphorus  
 455 activation and transformation at the sedimentwater interface during plant debris decomposition.  
 456 *Sci. Total Environ.* **2017**, *583*, 458-465.

457 41. Zhang, S.; Zhao, Y.; Zhou, C.; Duan, H.; Wang, G., Dynamic sulfur–iron cycle promoted  
 458 phosphorus mobilization in sediments driven by the algae decomposition. *Ecotoxicology* **2020**,  
 459 1-10.

460 42. Gao, H. L., Qian, X., Wu, H. F., Li, H. M., Pan, H., Han, C . M., Combined effects of  
 461 submerged macrophytes and aquatic animals on the restoration of a eutrophic water body-a  
 462 case study of Gonghu Bay, Lake Taihu. *Ecological Engineering* **2017**, *102*, 15-23.

463 43. Wang, J.; Jiang, X.; Zheng, B.; Chen, C.; Kang, X.; Zhang, C.; Song, Z.; Wang, K.; Wang,  
 464 W.; Wang, S., Effect of algal bloom on phosphorus exchange at the sediment-water interface  
 465 in Meiliang Bay of Taihu Lake, China. *Environ. earth Sci.* **2016**, *75*, (1), 57.

466 44. Cui, Y.; Jin, Z.; Wang, Y.; Guo, S.; Fu, Z.; Yang, Y.; Wang, Y., Mechanism of eutrophication  
 467 process during algal decomposition at the water/sediment interface. *J. Clean. Prod.* **2021**, *309*,  
 468 127157.

469 45. Yang, Q.; Wang, X.; Luo, W.; Sun, J.; Xu, Q.; Chen, F.; Zhao, J.; Wang, S.; Yao, F.; Wang,

470 D.; Li, X.; Zeng, G., Effectiveness and mechanisms of phosphate adsorption on iron-modified  
471 biochars derived from waste activated sludge. *Bioresource Technol.* **2017**, *247*, 537-544.  
472 46. Li, J.; Li, B.; Huang, H.; Lv, X.; Zhao, N.; Guo, G.; Zhang, D., Removal of phosphate from  
473 aqueous solution by dolomite-modified biochar derived from urban dewatered sewage sludge.  
474 *Sci. Total Environ.* **2019**, *687*, 460-469.

475